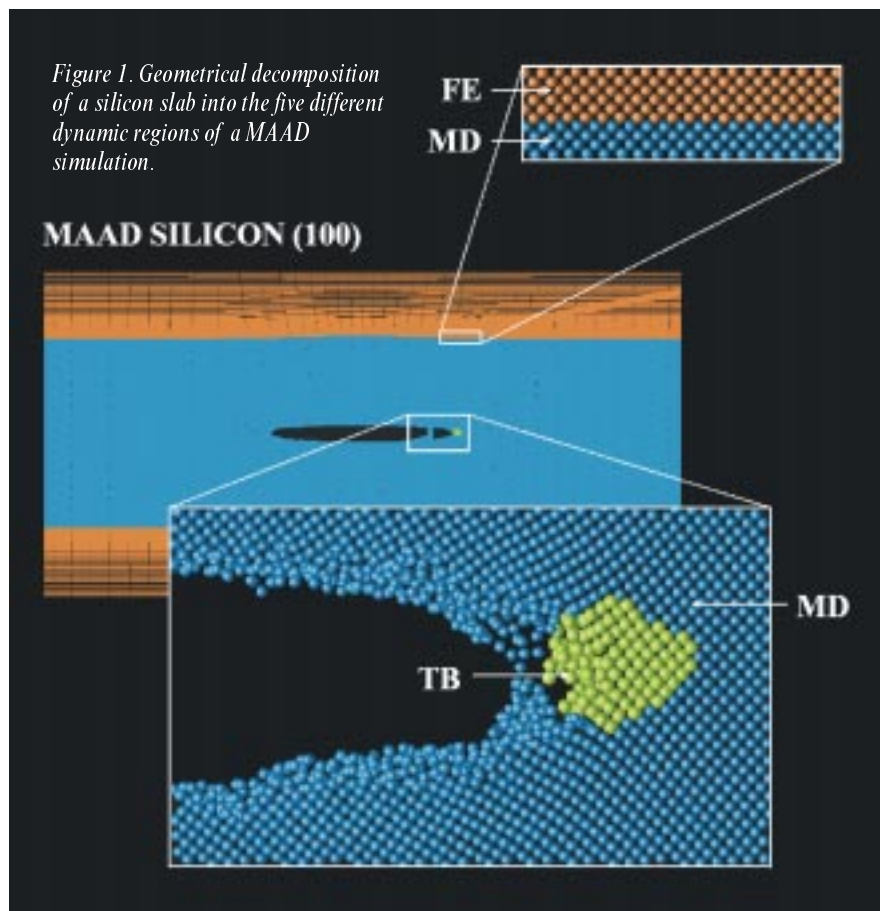


# Spanning the Length Scales in Dynamic Simulation

Farid F. Abraham,  
Jeremy Q. Broughton,  
Noam Bernstein, and  
Efthimios Kaxiras



**H**istorically, there is a rich tradition of attempting to couple different length and time scales in serial fashion. By this we mean that one set of calculations at a fundamental level, and of high computational complexity, is used to evaluate constants for use in a more approximate or phenomenological computational methodology at longer length or time scales.

In pioneering work of this sort in the 1980s, Clementi and coworkers<sup>1</sup> used high-quality quantum-mechanical methods to evaluate the interaction of several water molecules. From this database they parameterized an empirical potential for use in molecular-dynamics atomistic simulations. Such a simulation was then used to evaluate the viscosity of water from the atomic autocorrelation function. Finally, the computed viscosity was used in a computational-fluid-dynamics

calculation to predict tidal circulation in Buzzards Bay, MA. This *tour de force* of computational physics is a powerful example of the sequential coupling of length and time scales: one series of calculations is used as input to the next up the length and time hierarchy.

There are many other examples in the literature. But what underlies all these schemes is that an appropriate computational methodology is used for a given scale or task, whether it be the accuracy of quantum mechanics at the shortest scales or fluid dynamics at the longest scales. In contrast, there has been comparatively little effort devoted to the parallel coupling of different computational schemes for a simultaneous attack on a given problem; in our case, our interest dictates specific attention toward issues in materials or solid-state physics. We will focus specifically on the coupling of length scales for the three mechanics describing materials phenomena: quantum mechanics, atomistic mechanics, and continuum mechanics.

## Unified dynamical treatment

This challenging paradigm of computational science demands a unified dynamical treatment of a physical problem, in which the tools of engineering, physics, and chemistry are applied in a seamless formalism. We report such an accomplishment for the study of brittle fracture in silicon, though our approach has general applicability. In a single concerted

Farid F. Abraham is a research staff member in the IBM Almaden Research Center, San Jose, CA 95120. E-mail: farid@almaden.ibm.com

Jeremy Q. Broughton was a member of the research staff at the Complex Systems Theory Branch, Naval Research Laboratory, Washington, DC 20375, and is currently at the Yale School of Management.

Noam Bernstein was a graduate student in the Division of Engineering and Applied Sciences at Harvard University, Cambridge, MA 02138, and is currently at the Naval Research Laboratory, Washington, DC 20375.

Efthimios Kaxiras is a professor in the Department of Physics and the Division of Engineering and Applied Sciences at Harvard University, Cambridge, MA 02138.

simulation of dynamic fracture comprising the finite-element method, classical molecular dynamics, and quantum tight-binding dynamics, we demonstrate that spanning the length scales with dynamical bridges between the different physical descriptions is feasible. Our approach maps naturally onto scalable computer architectures.

The traditional approach for studying fracture is to adopt continuum mechanics,<sup>2,3</sup> the macroscopic view of matter. Because continuum mechanics allows material lengths to go to zero, there is no natural small-length cutoff, such as the size of an atom. Hence, a failure mechanism describing the loss of local material cohesion (for example, void formation) does not arise naturally from this macroscopic description. At the finer level of description of classical atoms interacting through empirical force laws, material decohesion does arise naturally,<sup>4,5</sup> and we choose to label this length scale the mesoscopic regime. We can even go one level finer. Treating bond breaking with an empirical potential may be unreliable, and a quantum-mechanical treatment may be desired. This *ab initio* level of description we call the microscopic regime. And if the crack is moving, a unified macroscopic, atomistic, *ab initio* dynamics (MAAD) description must be brought together into a seamless union, embracing all the size scales, from the very small to the very big. We now describe an implementation of such a program.

### Application to silicon

Our MAAD simulation is composed of computational procedures formulated in terms of a spatial decomposition of the system and has an obvious applicability for parallel processing. Our study is the rapid brittle fracture of a silicon slab flawed by a

microcrack at its center and under uniaxial tension. Figure 1 shows the geometrical decomposition of the silicon slab into the five different dynamic regions of the simulation: the continuum finite-element (FE) region; the atomistic molecular-dynamics (MD) region; the quantum tight-binding (TB) region; the FE-MD “handshaking” region; and the MD-TB “handshaking” region. The image is the simulated silicon slab, with expanded views of the FE-MD (orange nodes and blue atoms) interface and the TB (yellow atoms) region surrounded by MD (blue) atoms. Note that the TB region surrounds the crack tip with broken-bond MD atoms trailing behind this region. Only a proportion of the FE and MD regions is shown, since their extent is large.

The exposed notch faces are  $x$ - $z$  planes with (100) faces, with the notch pointed in the  $\langle 010 \rangle$  direction. There are 258,048 mesh points in each FE region, 1,032,192 atoms in the MD region, and approximately 280 unique atoms in the TB region. The lengths of the MD region are 10.9 Å for the slab thickness, 3649 Å in the primary direction of propagation, and 521 Å in the direction of pull (before pulling). Periodic boundary conditions are imposed at the slab faces normal to the direction of thickness and to crack propagation. The full pull length of the FE+MD system is 5602 Å. In our studies, the time for a TB force update was 1.5 s, that for the MD update was 1.8 s, and that of the FE update was 0.7 s. We could thus afford to double the size of the FE region in order to accomplish computational load balancing but

*A computational approach to the simulation of crack propagation in silicon seamlessly unites quantum, atomistic, and continuum descriptions of matter*

## Ingredients of the Finite-Elements Technique

In the finite-elements (FE) technique, the continuum elastic energy (which is a function of the displacement field, a continuous variable) is integrated over the entire volume of the sample by placing a mesh over the system. If the displacements are known at the mesh points (nodes), then interpolation can be used within each element (cell) of the mesh to determine the displacement field everywhere. The elastic-energy integral is then replaced by a sum over cells (triangles in two dimensions, tetrahedra in three dimensions), and the important dynamical variables in the problem are the values of the displacements at the nodes. The kinetic-energy integral is handled similarly.

Since an energy is defined for the FE region, forces on the dynamical variables can be obtained. Thus, the time evolution of the system may be propagated in the same way as in molecular dynamics (MD). In the FE/MD handshake region, it is important to have FE mesh points coincident with the ideal atomic sites of the MD region; thus it is academic whether we think of these sites as representing atoms or nodes.

The Hamiltonian, without body forces or tractions, is defined by

$$E = \frac{1}{2} \int dV \varepsilon_{\mu\nu} C_{\mu\nu\lambda\sigma} \varepsilon_{\lambda\sigma} + \frac{1}{2} \int dV \rho |\dot{u}|^2,$$

where  $\varepsilon$  is the strain tensor,  $C$  is the elastic-constant matrix,  $\rho$  is the density, and  $\dot{u}$  is the time derivative of the displacement field. The interpolation of a function within the finite-element cell is defined by

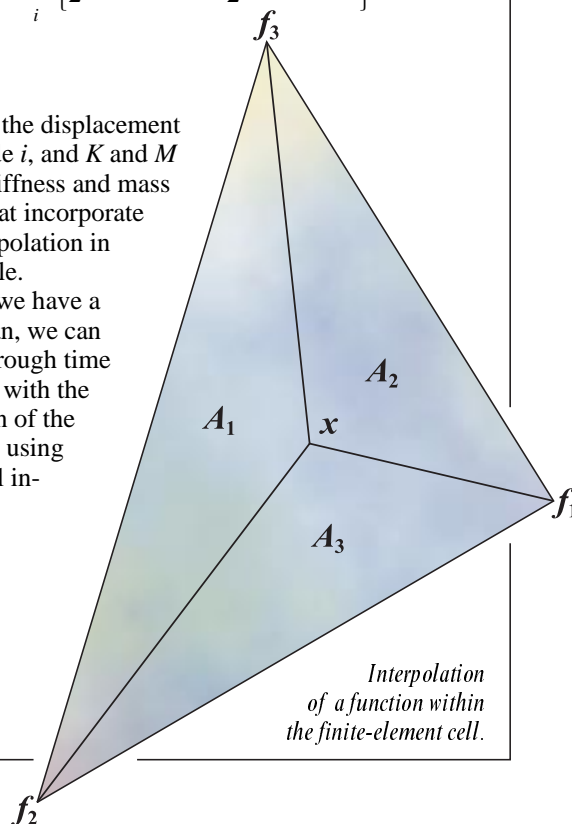
$$f(x) = (A_1 f_1 + A_2 f_2 + A_3 f_3) / (A_1 + A_2 + A_3),$$

where  $f_i$  is the value of the function at node  $i$  and  $A_i$  is the corresponding area (as shown in the figure). Performing the integral over each cell yields the energy evaluated on the mesh

$$E = \sum_i^{\text{#cells}} \left\{ \frac{1}{2} u_{\alpha}^i K_{\alpha\beta}^i u_{\beta}^i + \frac{1}{2} \dot{u}_{\alpha}^i M_{\alpha\beta}^i \dot{u}_{\beta}^i \right\},$$

where  $u^i$  is the displacement field at node  $i$ , and  $K$  and  $M$  are local stiffness and mass matrices that incorporate linear interpolation in each triangle.

Since we have a Hamiltonian, we can advance through time in lockstep with the MD portion of the simulation, using an identical integrator.



without any sacrifice of wall-clock time. The TB region was relocated after every 10 time steps.

In the “far-field” regions, we have a continuum treated by the well-known FE procedure<sup>6</sup> (see “Ingredients of the Finite-Elements Technique,” above). This macroscopic description merely needs the constitutive law for the material. One processor is used for each of the two FE regions.

Around the crack, with large strain gradients but with no bond rupture, we use the classical MD method to treat the highly nonlinear deformation on the atomic scale (see “Ingredients of the Molecular-Dynamics Technique,” p. 542). Molecular dynamics predicts the motion of the atoms governed by their mutual interatomic interactions and requires the numerical integration of the Newton’s classical equations of motion. The Stillinger-Weber (SW) potential<sup>7</sup> is taken to represent the empirical force law between the silicon atoms. Because MD has a large computational burden, we partition this region spatially onto several processors (24 in the present example).

Lastly, in the region of bond failure at the crack tip, we use the TB formalism, which is a semiempirical electronic-structure description of matter. It is one of the fastest numerical quantum methods containing electronic-structure information. Rather than evaluating costly integrals, it uses predetermined parameterized matrix elements for the material under study. For this silicon study, we employed the nonorthogonal TB scheme due to Bernstein and Kaxiras.<sup>8</sup> The nuclei are treated as classical point objects. Because the TB region is the most computationally demanding part of the overall code, small TB regions must be used so as to allow overall load balancing. We tracked the path of the crack and placed the center of the TB region at the apex of the crack where the bond breaking occurs.

For extended regions of bond rupture, we used overlapping TB regions taken to be a “clover leaf” of (eight) overlapping TB regions, each being cylindrical and distributed to a different processor. Each of the eight TB regions is a cylinder with radius 5.43 Å in the  $y$ - $z$  plane. The force on an atom

residing in more than one of the overlapping TB regions was taken to be the average value.<sup>9</sup> The total number of unique “clover-leaf” atoms is therefore less than the sum of all of the atoms in the eight TB regions. For small deformations, overall consistency was ensured by making sure that the linear elastic constants in all three regions were the same. We also found from calculation that the elastic modulus of silicon using the empirical SW potential is almost identical to the prediction of TB for strains up to the mechanical stability limit of the bulk solid. For more on the subject, see “Ingredients of the Tight-Binding Technique,” p. 544.

---

*The overarching theme is  
that a Hamiltonian  $H_{\text{Tot}}$  is defined  
for the entire system.*

---

The overarching theme is that a Hamiltonian  $H_{\text{Tot}}$  is defined for the entire system. Its degrees of freedom are atomic positions  $\mathbf{r}$  and their velocities  $\dot{\mathbf{r}}$  for the TB and MD regions, and displacements  $\mathbf{u}$  and their time rates of change  $\dot{\mathbf{u}}$  for the FE regions. (The velocities and conjugate momenta are simply related.) Equations of motion for all the relevant variables in the system are obtained by taking appropriate derivatives of this Hamiltonian. All variables can then be updated in lockstep as a function of time using the same integrator. Thus the entire time history of the system may be obtained numerically given an appropriate set of initial conditions. Conceptually,  $H_{\text{Tot}}$  may be written:

$$\begin{aligned}
 H_{\text{Tot}} = & H_{\text{FE}}(\{\mathbf{u}, \dot{\mathbf{u}}\} \in \text{FE}) + H_{\text{FE/MD}}(\{\mathbf{u}, \dot{\mathbf{u}}, \mathbf{r}, \dot{\mathbf{r}}\} \in \text{FE/MD}) \\
 & + H_{\text{MD}}(\{\mathbf{r}, \dot{\mathbf{r}}\} \in \text{MD}) + H_{\text{MD/TB}}(\{\mathbf{r}, \dot{\mathbf{r}}\} \in \text{MD/TB}) \\
 & + H_{\text{TB}}(\{\mathbf{r}, \dot{\mathbf{r}}\} \in \text{TB})
 \end{aligned}$$

This equation should be read as implying that there are three separate Hamiltonians for each subsystem as well as Hamiltonians that dictate the dynamics of variables in the handshake regions. “MD/TB” and “FE/MD” imply such handshake regions. Following a trajectory dictated by this Hamiltonian will result in a conserved total energy. This is an important feature of our computational approach, since it ensures numerical stability.

### Hand-shaking algorithms

Two crucial aspects of our MAAD procedure are the handshaking algorithms between the FE and the MD regions and between the MD and the TB regions. In both cases, seamless couplings are required.<sup>9,10</sup>

In the FE/MD handshake region (see Fig. 2), the FE mesh spacing is scaled to atomic dimensions. Moving away from the FE/MD region and deep into the continuum, we can expand the mesh size. Thus we can embed our atomistic simulation in a large continuum solid. FE cells contributing

fully to the overall Hamiltonian (unit weight) are marked with heavy lines. FE cells contributing to the handshake Hamiltonian (half weight) are represented by light lines. Two- and three-body terms (dotted lines) of SW interactions that cross the boundary also carry half weight. Continuous lines represent unit-weight SW interactions. The FE region has displacements associated with each mesh point; these displacements follow a Hamiltonian given by continuum linear-elasticity theory. We employ an update algorithm identical to that used in conventional MD so that the displacements now are dy-

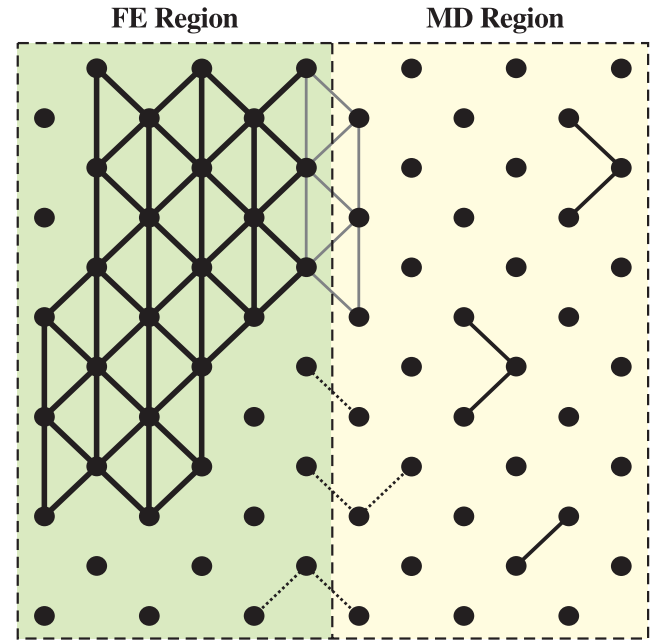


Figure 2. Illustration of FE/MD handshake Hamiltonian (see text).

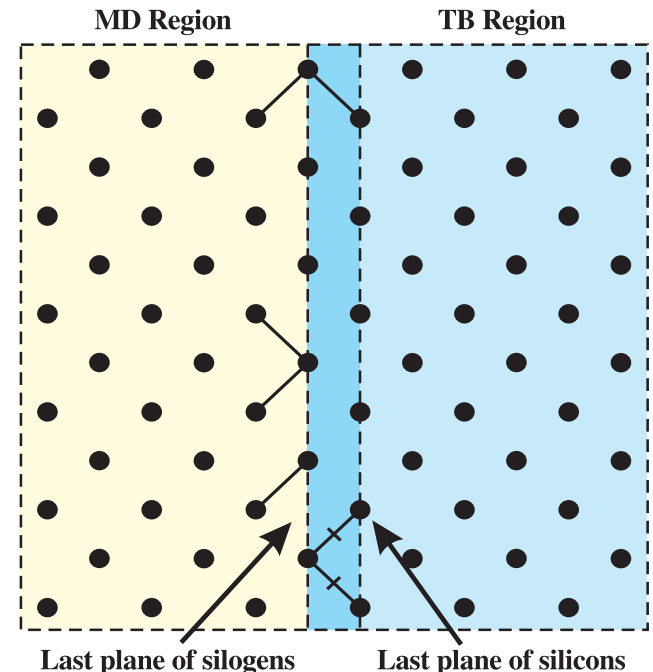


Figure 3. Illustration of MD/TB handshake Hamiltonian (see text).

## Ingredients of the Molecular-Dynamics Technique

In the molecular-dynamics (MD) technique, atoms are propagated through space and time using Newton's laws of motion. At most ambient temperatures and for most elements, a classical (as opposed to quantum) description of the dynamics of atomic motion is perfectly satisfactory. All that is required is an interatomic force law.

For silicon, many force laws have been parameterized against experimental observables. We chose that due to Stillinger and Weber.<sup>1</sup> It writes the total potential energy of the system as a sum over pairs of atoms plus a sum over triplets of atoms. The pair sum represents bonds between atoms and is a function of their separation. The triplet sum describes bond-bending terms and is a function of the angle between pairs of bonds centered on any given atom. In a

covalent solid such as silicon, the bond-bending terms are important; they are what differentiate the structural properties from those of a metal. Forces, required for the MD position-update algorithm, are obtained from derivatives of the potential energy.

The Hamiltonian consists of the normal kinetic energy

$$E_k = \sum_i^{\text{atoms}} \frac{1}{2} m |v_i|^2$$

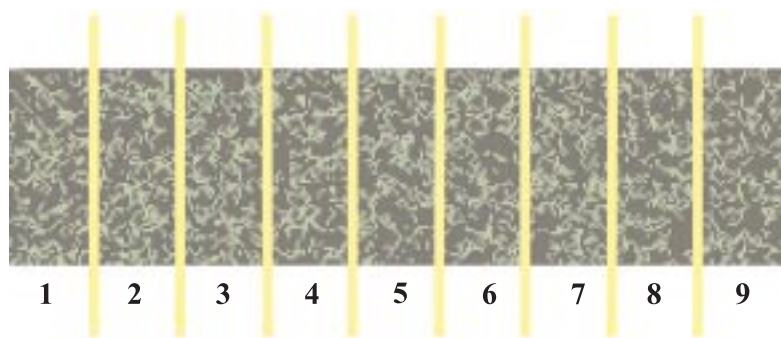
plus a potential energy defined by the function

$$E_p = \sum_{ij}^{\text{pairs}} V^{(2)}(r_{ij}) + \sum_{ijk}^{\text{triplets}} V^{(3)}(r_{ij}, r_{jk}, \theta_{ijk}),$$

where  $r_{ij}$  is the distance between atoms  $i$  and  $j$ ,  $\theta_{ijk}$  is the angle between bonds  $i-j$  and  $j-k$ ,  $V^{(2)}$  is the pair potential, and  $V^{(3)}$  is the three-body potential.

The equations of motion are integrated with respect to time using a multiple-time-step algorithm based on a Trotter expansion of the Liouville operator.<sup>2</sup> The code is parallelized using a one-dimensional (1D) domain decomposition (shown in the figure); data flow via a 1D shift operator.

MD SYSTEM



PROCESSOR NUMBER

*One-dimensional domain decomposition parallelizes MD code.*

## References

1. F. H. Stillinger and T. A. Weber, "Computer simulation of local order in condensed phases of silicon," *Phys. Rev. B* **31**, 5262-5271 (1985).
2. M. Tuckerman, B. J. Berne, and G. J. Martyna, *J. Chem. Phys.* **97**, 1990 (1992).

namical variables that follow in lockstep with those of their atomic cousins in the MD region.

The FE/MD interface is chosen to be far from the fracture region; hence, atoms and the displacements of the FE lattice can be unambiguously assigned to one another. This is accomplished by taking the interactions across the FE/MD boundary to be the mean of the FE Hookean description and the MD interatomic-potential description.

For the MD/TB handshake interface (see Fig. 3), dangling bonds at the edge of the TB region are terminated with pseudohydrogens; we add "pseudo-" because the matrix elements are carefully constructed to tie off a single bond and ensure no charge transfer when that atom is placed in a position commensurate with the silicon lattice. Conceptually, the TB terminating atoms are monovalent silicons, hence the term "silogen" used in Fig. 3.

The TB Hamiltonian is diagonalized for the sum of light plus dark blue regions in Fig. 3. Silicon-silicon matrix elements are employed in the light-blue area, and silicon-silogen

matrix elements are used in the dark-blue region. Two- and three-body SW interactions contributing to the handshake Hamiltonian are designated by full lines. Broken lines represent noncontributing SW three-body terms. Only representative SW examples are shown.

Thus, at the perimeter of the MD/TB region, we have silogens that sit directly on top of the atoms of the MD simulation. We imagine that on one side of the TB/MD interface, the bonds to an atom are derived from the TB Hamiltonian and that on the other side, they are derived from the interatomic potential of the MD simulation. As before, the TB code updates atomic positions in lockstep with its FE and MD cousins. The entire MAAD procedure is formulated in such a way that the system, in the absence of dynamic TB tracking of the crack front, follows a conservative Hamiltonian. A detailed discussion of the MAAD techniques is in preparation.<sup>9</sup>

## Details of fracture simulation

We give some important details of the MAAD simulation

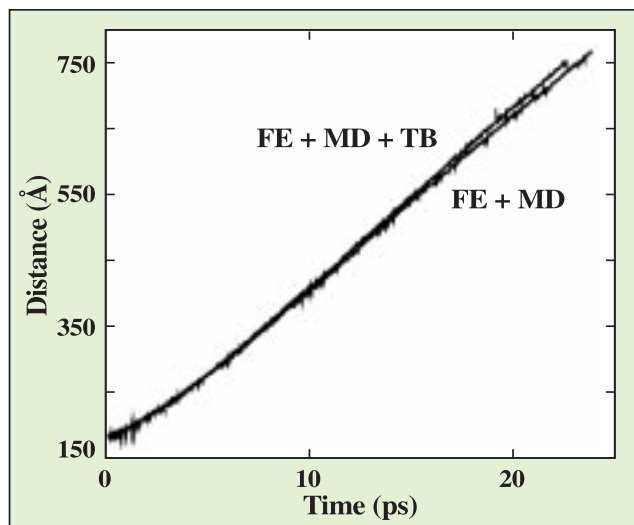


Figure 4. Distance-versus-time history of the two crack tips, one having the TB atoms always centered at the immediate failure region.

of silicon fracture (see Fig. 1). The slab is initialized at zero temperature, and a constant strain rate is imposed on the outermost FE boundaries, defining the opposing horizontal faces of the slab. A linear velocity gradient is established across the slab; hence, an increasing strain with time occurs in the solid slab. The solid fails at the notch tip when the solid has been stretched by approximately 1.5%. The imposed strain rate is then set to zero at the onset of crack motion. Figure 4 presents the history of distance versus time for the two crack tips, one having the TB atoms dynamically centered

at the immediate failure region. The two propagating crack tips rapidly achieve a limiting speed of 2770 m/s, which is equal to 85% of the Rayleigh speed, the sound speed at the solid silicon surface. The two distance-time histories are nearly identical. In hindsight, this might have been expected, since the elastic moduli of silicon calculated from the empirical SW potential and from TB are nearly the same up to the mechanical-stability limit of the bulk solid. More important, this indicates that the handshaking between the MD region and the TB region is reliable.

In Fig. 5, the stress propagating through the slab is revealed with the help of a finely tuned potential-energy color scale. Note that the stress waves are passing from the MD region to the FE regions with no visible reflection at the FE-MD interface; that is, the coupling of the MD region with the FE region appears seamless. In Fig. 6, we see that the straight-ahead brittle cleavage of the silicon slab leaves behind surfaces that show an increasing roughening with crack distance. The origin of this observed surface roughening is consistent with a suggestion by Rice,<sup>11</sup> which we now explain.

*The entire time history of the system may be obtained numerically given an appropriate set of initial conditions.*

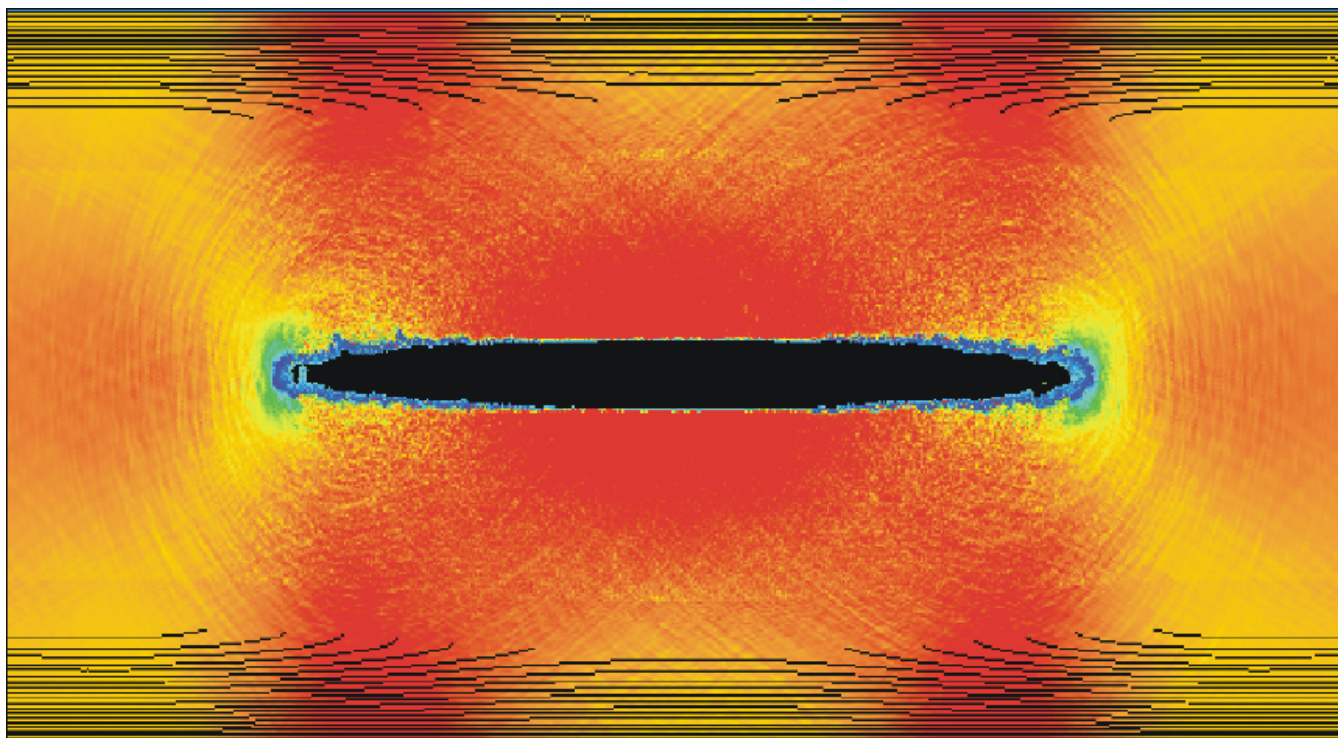
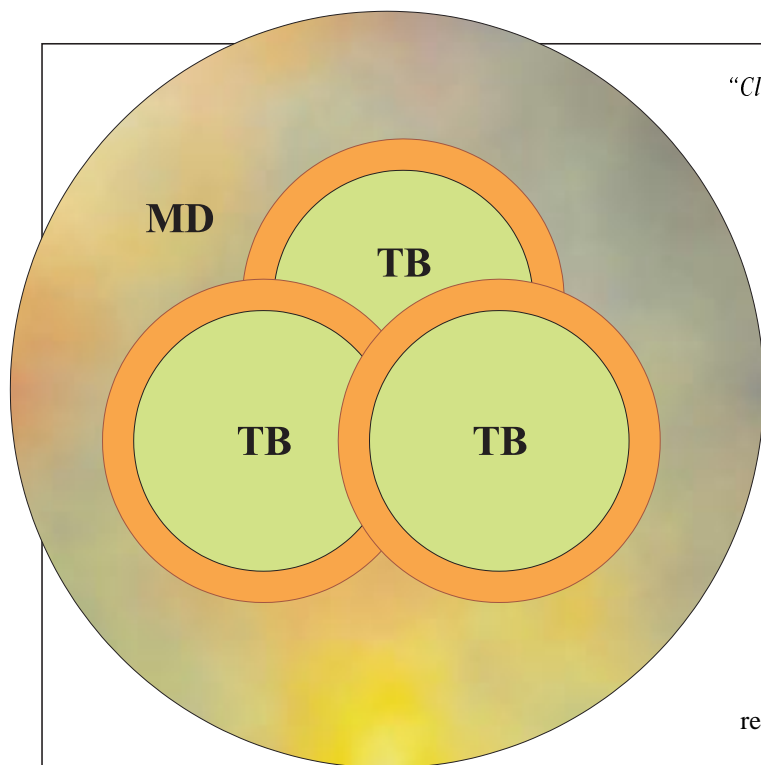


Figure 5. Stress waves propagating through the slab, revealed with the help of a finely tuned potential-energy color scale.



“Clover leaf” of overlapping TB volumes represents the entire TB region.

## Ingredients of the Tight-Binding Technique

In the tight-binding (TB) technique, the energy of the system is written as an eigenvalue sum plus interatomic pairwise terms. The eigenvalues are parameterized to be as close as possible to those of an *ab initio* quantum-mechanical calculation. The sum is over occupied one-electron states up to the Fermi level. The parameterization is of the elements that constitute the TB Hamiltonian matrix. This matrix has to be diagonalized at every time step of the simulation—that is, for every configuration of atoms in the TB region. Since diagonalization is  $O(N^3)$  computationally expensive, this is the most computationally complex part of the whole coupled algorithm. Each matrix element is a function of (a) the distance between pairs of atoms and (b) the basis function sitting on either site. Each silicon has one *s* and three *p* atomic-basis orbitals.

Another term in the total energy originates because, in *ab initio* one-electron theories such as Hartree-Fock or density-functional theory, the total energy is not just an eigenvalue sum; it has additional terms due to double counting of Coulomb integrals and exchange-correlation terms. To a good approximation, these can be parameterized via a pairwise sum. As with the finite-elements and molecular-dynamics (MD) regions, forces are obtained from derivatives of the energy. The atoms in the TB region can be updated in lockstep with the rest of the system.

In the MD/TB handshake region, the bonds dangling from the surface of the embedded TB cluster are terminated with monovalent “atoms” that we call “silogens.” These silogens are constrained to be coincident

with the silicon atoms on the inner perimeter of the MD region. The coupling may therefore be envisaged as a TB cluster residing in an MD void but with the outer TB silogens sitting on top of the inner MD silicon atoms. Careful bookkeeping in the handshake region accounts for all the bonds. Each silogen has a single *s* atomic-basis orbital.

The TB matrix is thus  $(4N_{\text{in}} + N_{\text{out}})^2$  in size, where  $N_{\text{in}}$  represents the number of silicons and  $N_{\text{out}}$  represents the number of silogens in each TB region.

Because the TB algorithm has high computational complexity, we chose to represent the entire TB region as a “clover leaf” of overlapping TB volumes (shown in the figure). Forces employed for propagation of atoms in overlapping regions are taken to be the average of those calculated in the superposed TB volumes.

The Hamiltonian consists of the same kinetic energy as for MD plus a potential energy defined by

$$E_p = \sum_n^{\text{#occ}} \epsilon_n + \sum_{ij}^{\text{pairs}} \varphi(r_{ij}),$$

where  $\epsilon_n$  is the eigenvalue of state  $n$ , the first sum is carried out over the occupied electronic states, and  $\varphi(r_{ij})$  is the pairwise interaction between atoms  $i$  and  $j$ . The eigenvalues are calculated by solving the matrix equation

$$\mathbf{H}\Psi_n = \epsilon_n \mathbf{S}\Psi_n$$

where  $\mathbf{H}$  is the electronic Hamiltonian matrix,  $\mathbf{S}$  is the overlap matrix, and  $\Psi_n$  is the eigenvector of state  $n$ .

The matrix elements

$$H_{lm} = \langle \phi_l | \mathbf{H} | \phi_m \rangle$$

$$S_{lm} = \langle \phi_l | \phi_m \rangle$$

are computed within the two-center approximation and decay smoothly to zero as the interatomic separation  $r$  reaches a cutoff distance  $r_c$ . Solving the generalized eigenvalue problem yields the forces that are the expectation values of derivatives of  $\mathbf{H}$  and  $\mathbf{S}$ .

The TB dynamics is advanced in lockstep with the MD portion of the simulation, using the same time integrator.

There are two “generic” classes of materials failure: brittle and ductile (see “Failure of Ductile and Brittle Materials,” p. 546). In brittle failure, a crack propagates by atomic-bond cleavage and the creation of surfaces. In ductile failure, plastic deformation occurs by the motion of rows of atoms sliding past one another on preferred slip planes (dislocations).

By comparing Griffith’s condition for brittle fracture and the criterion of unstable stacking-fault energy for dislocation emission (ductile failure), Rice<sup>11</sup> predicted that diamond cubic crystals such as silicon (Si) and germanium are more likely to emit dislocations than some face-centered cubic (fcc) metals such as iridium. Iridium, although known to cleave, can nevertheless show substantial dislocation activity. However, in contrast to theoretical predictions, silicon and germanium are known experimentally to be brittle materials. Rice speculated that “While ... Si should show dislocation nucleation from a crack tip at low temperatures ..., the low mobility of any such dislocations, once nucleated, may condemn Si even then to a brittle response.”<sup>11</sup>

Our simulation confirms Rice’s idea. We suggest that the spawning of dislocations with low mobility on the time scale of the crack motion would likely manifest itself as an atomic-scale roughening of the freshly cleaved surfaces; that is, a proliferation of nucleated dislocations would *freeze upon emission* and result in surface disorder. Such nucleation of mobile dislocations was observed in previous simulations of fcc failure (see “Failure of Brittle and Ductile Materials,” p. 546, and Ref. 4).

### Future prospects

We have chosen an “ideal” problem, brittle fracture, applied to an “ideal” system, silicon, to illustrate the MAAD-simulation approach to spanning the length scales. Further applications are being pursued, including dynamical apportioning of TB processors to multiple regions of the physical system (for example, if crack branching occurs). We wish to emphasize that although progress has been achieved, we view our effort as only a beginning to a new and obviously challenging endeavor. Improved techniques for the three mechanics will be applied, and more robust procedures for interfacing the three regimes will be invented. We believe that applications will only be limited by the imagination of the researcher.

### Acknowledgments

We acknowledge support from the U.S. Air Force Research Laboratory’s Maui High Performance Computing Center, which is administered by the University of New Mexico. FFA thanks X. P. Xu for early participation and H. Gao for discussions. JQB wishes to acknowledge support of the Office of Naval Research and DARPA and to thank the Department of Defense’s HPCMO for a “Grand Challenge” award. We wish to thank the National Science Foundation (NSF) and the ITP at Santa Barbara for support and hospitality. NB is supported by Harvard’s Materials Research Science and Engineering Center, which is funded by NSF.

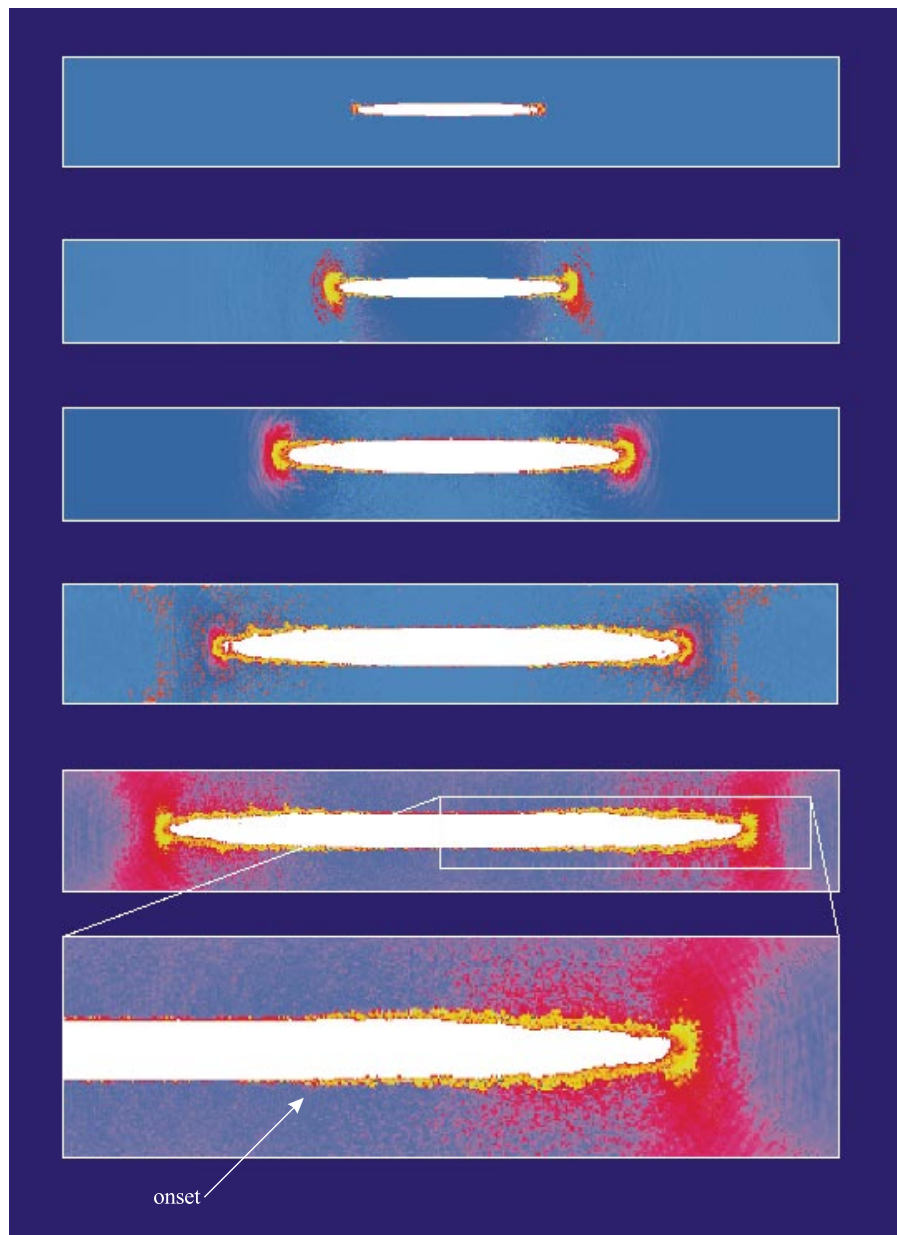


Figure 6. Roughening of the solid silicon surfaces increases with growing crack length. The onset of surface roughening is shown in an expanded view.

## Failure of Brittle and Ductile Materials

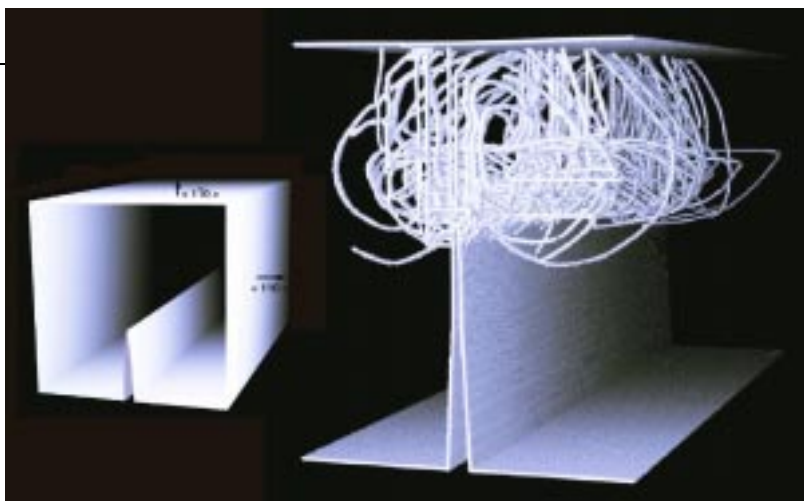
In the simulation of silicon failure, we observe features associated with rapid brittle fracture. Brittle fracture certainly is not the sole mechanism for the failure of materials when they are hit hard and fast; otherwise, our world would be quite fragile.

The two generic classes describing materials failure are "brittle" and "ductile." In the first case, chemical bonds are broken; this is what happens when glass shatters. In ductile failure, such a catastrophic event does not occur. "Tough" materials like metals do not shatter; they bend because plastic deformation occurs by the motion of rows of atoms sliding past one another on preferred "slip planes" (dislocations), in contrast to bond breaking. That is why car fenders are not made of brittle materials like glass. The two general classes of failure do not depend on the details of the interatomic interactions, but they do depend on the atomic packing of the three-dimensional solid. The interatomic potential dictates the packing.

The number of atomic packings in nature is limited. Glasses do not have extended crystallinity; instead, the atoms in glasses are packed randomly. Glasses have no "slip planes" and therefore cannot exhibit ductility arising from atomic planes sliding past one another.

Crystals do not have the isotropy of glasses. In a sense a crystal is defective in view of the loss of perfect isotropy, the defect being multiplanar and infinite in extent! Because of the "breaking" of the perfect isotropic symmetry, slip planes exist, dislocations are possible, and ductility may win out over brittle failure.

The face-centered-cubic packing is known to have a



Rare-gas solid exhibits dynamic ductile failure in this MD simulation.

strong propensity toward ductility. However, the lack of slip planes and the inability to characterize dislocations in an amorphous or glassy material do not in themselves exclude ductile behavior. Metallic glasses can exhibit plastic failure. Also, crystallinity does not assure ductility; strongly covalent solids tend to be brittle.

The figure depicts a molecular-dynamics simulation of dynamic ductile failure of a rare-gas solid. The model system is a three-dimensional slab having a total of 100,509,696 atoms. Only those atoms that have a cohesive energy less than 97% of the ideal bulk value are shown, which reduces the number of atoms seen by approximately two orders of magnitude. The small box shows the notched solid before uniaxial stretching is applied in the  $\langle 110 \rangle$  direction. After stretching, a "flower" of loop dislocations blossoms from the crack tip, and elastic energy continues to dissipate through the continued creation and motion of dislocations. [See F. F. Abraham *et al.*, *J. Mech. Phys. Solids* **45**, 1461–1471 (1997).]

## References

1. E. Clementi, "Global scientific and engineering simulations on scalar, vector and parallel LCAP-type supercomputers," *Philos. Trans. R. Soc. London, Ser. A* **326**, 445–470 (1988).
2. A. H. Cottrell, *The Mechanical Properties of Matter* (Wiley, New York, 1964). This wonderful, out-of-print book is not outdated.
3. L. B. Freund, *Dynamical Fracture Mechanics* (Cambridge University Press, New York, 1990).
4. F. F. Abraham *et al.*, "Instability dynamics of fracture: a computer simulation investigation," *Phys. Rev. Lett.* **73**, 272–275 (1994); F. F. Abraham *et al.*, "Instability dynamics in three-dimensional fracture: an atomistic approach," *J. Mech. Phys. Solids* **45**, 1461–1471 (1997).
5. A. Nakano, R. K. Kalia, and P. Vashishta, "Dynamics and morphology of brittle cracks: a molecular dynamics study of silicon nitride," *Phys. Rev. Lett.* **75**, 3138–3142 (1995); A. Omeltchenko *et al.*, "Crack front propagation and fracture in a graphite sheet: a molecular-dynamics study on parallel computers," *Phys. Rev. Lett.* **78**, 2148–2152 (1997).
6. T. Hughes, *The Finite Element Method* (Prentice Hall, Upper Saddle River, NJ, 1987).
7. F. H. Stillinger and T. A. Weber, "Computer simulation of local order in condensed phases of silicon," *Phys. Rev. B* **31**, 5262–5271 (1985).
8. N. Bernstein and E. Kaxiras, "Nonorthogonal tight-binding Hamiltonian for defects and interfaces in silicon," *Phys. Rev. B* **56**, 10488–10496 (1997).
9. J. Q. Broughton, N. Bernstein, E. Kaxiras, and F. F. Abraham, in preparation.
10. An early suggestion for coupling the continuum and atomistic regimes was given by W. G. Hoover, A. De Groot, and C. Hoover, "Massively parallel computer simulation of plane-strain elastic-plastic flow via nonequilibrium molecular dynamics and Lagrangian continuum mechanics," *Comput. Phys.* **6**, 155–167 (1992). A very recent study describing a method for interfacing these two regimes is H. Rafii-Tabar, L. Hua, and M. Cross, "A multiscale atomistic-continuum modelling of crack propagation in a two-dimensional macroscopic plate," *J. Phys. Cond. Matter* **10**, 2375–2387 (1998). A nondynamical formalism bringing atomic information into the continuum mechanics of deformation is described by V. Shenoy *et al.* in "Quasicontinuum models of interfacial structure and deformation," *Phys. Rev. Lett.* **80**, 742–745 (1998). In a paper by R. Capaz, K. Cho, and J. Joannopoulos, "Signatures of bulk and surface arsenic antisite defects in GaAs(110)" [*Phys. Rev. Lett.* **75**, 1811–1814 (1995)], an atomistic/tight-binding coupling scheme is employed to predict equilibrium structure. A review of the issues involved in coupling quantum systems to classical force fields is given by P. T. Vanduijn and A. H. Devries, "Direct reaction field force field: A consistent way to connect and combine quantum-chemical and classical descriptions of molecules," *Int. J. Quant. Chem.* **60**, 1111–1132 (1996). We are unaware of any study coupling all three regimes either concurrently or dynamically. A more complete discussion of various published schemes will be provided in Ref. 9.
11. J. R. Rice, "Dislocation nucleation from a crack tip: an analysis based on the Peierls concept," *J. Mech. Phys. Solids* **40**, 239–271 (1992).